

Temporal and ear imaging: normal or abnormal findings?

Ferdinando Calzolari

Former director of the Neuroradiology Department of the University Hospital of Udine (Italy)
ferdinando.calzolari@gmail.com

Abstract

The temporal bone is known as an area of complex anatomy.

In routine diagnostic imaging the tiniest structures may be occult or poorly visualized, especially by radiologists and clinical doctors not particularly skilled in temporal bone imaging. Doubtful findings, small bony structures, thin canals and fine sutures cause sometimes problems in the differentiation between normal and abnormal situations; anatomical variants should not be confused with pathological structures. So, recognize the existence of infrequent or not so evident findings requires robust knowledge of this regional anatomy, regarding not only the bone structures, but also the nervous and vascular ones. Moreover, familiarity with embryological and developmental notions may help to diagnose physiological aspects or anatomical variants.

The aim of this paper is not an exhaustive description of each temporal bone structure and all possible anatomical variants in this region, but to remind some particular ear and temporal radiological findings which can imply problems of differential diagnosis or, on the other hand, which should be described for justify the symptoms, report any dangers of complications in case of pathology or alert the surgeon if surgical therapy is needed.

Keywords: temporal bone, anatomy, ear, canals, arteries, veins, nerves, sutures.

Introduction

The temporal bone includes five distinct bone components defined as mastoid, petrous, squamous, tympanic and styloid (Kwong et al. 2012, 428). These segments within the skull base contain small, numerous and critical structures, such as external, middle and inner ear components, nerves, arteries and veins (Isaacson 2018, 321). The analysis of temporal "microanatomy" imaging often implies discomfort and worry among radiologist not particularly expert on this field (Benson et al. 2019, 209). Diagnostic doubts may arise from the lack of knowledge of the development and particularities of these anatomical structures in relation to age. Small bony structures, thin canals and fine sutures cause sometimes problems not only of visualization and interpretation, but also of differentiation between normal and abnormal findings; anatomic variants should not be

confused with pathological structures (Koesling et al. 2005, 335). Moreover, some findings could be occult or misinterpreted also by audiologists and otolaryngologists who view the images in second instance.

Precise and complete imaging of the temporal bone and in particular of the ear is necessary not only to diagnose pathological pictures and to give an indication of the eventual aesthetic and audiological therapy, but also to plan surgical treatment and avoid iatrogenic lesions.

The purpose of this paper is to describe some doubtful or not so frequent computed tomography (CT) and magnetic resonance imaging (MRI) findings concerning the ear and the temporal bone that may involve recognition, interpretation or differential diagnosis problems. In particular, ear findings in pedi-

atric age and others concerning nervous and vascular structures are described.

MRI and CT findings

1 Pediatric age

In recent years there has been a notable increase in neuroradiological investigations in infants and children, largely due to advances in imaging equipment and anesthesiology procedures. Moreover, early diagnostics in cochlear implant candidates has contributed to increasing the number of MRI and CT performed in pediatric age, especially in the first months of life.

1.a Middle ear and mastoid cavities

MRI is highly sensitive for detecting inflammatory tissue and effusion in temporal cavities. On MRI of the brain, the middle ears and mastoid cavities are routinely included in the field of view, and very often abnormal signal intensities are seen inside them, particularly in first years of life. Radiologists usually describe these as incidental findings, but the clinical meaning of these incidental abnormalities on MRI remains controversial (Balci et al. 2008, 1850).

Anyway, regardless of whether it is panoramic cranial-encephalic examinations or targeted studies of the posterior cranial fossa, of the temporal region and in particular of the ear, it is necessary to point out some differences in the MRI signal between middle ear and mastoid. In infants aged < 1 year, particularly in the first 20 weeks of life, abnormal intensities in the middle ear such as low signal intensity on T1-weighted images and high signal intensity on T2-weighted images usually indicate liquid effusion. Otherwise abnormal intensities in the mastoid region usually demonstrated intermediate signal intensities on both T1- and T2-weighted images; this intermediate intensity on MRI probably indicates bone marrow (Figure 1a). In fact, histopathological studies of the temporal bone reported that the mastoid cavity is not completely formed until birth and that the mastoid cavity develops gradually after birth (Sano et al. 2007, Basraoui et al. 2018, 21). CT, nowadays rarely performed in newborn and infants, confirm mastoid structures without or with small aerated cells (Figure 1b).

Signal of liquid or effusion inside the middle ear does not always correspond to an inflammatory picture, albeit asymptomatic.

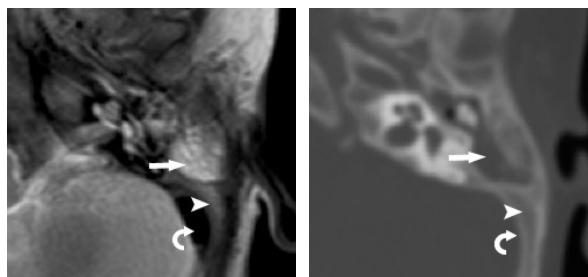


Figure 1
6-month-old male. a) MRI, axial T2-weighted image. Hyperintense tissue in the middle ear and mastoid antrum, possibly due to exudative fluid or mesenchyme (arrow). Intermediate intensity signal in the mastoid region indicates bone marrow (arrowhead). Compact cortical bone has no signal (curved arrow). b) CT, corresponding axial image. Liquid effusion or mesenchyme (arrow), mastoid bone marrow (arrowhead), hyperdense cortical bone (curved arrow).

Amniotic fluid may be present at birth in the middle-ear cavity (Priner et al. 2003). This fluid can be incidentally detected on brain MRI performed during the first days of life, usually in case of perinatal encephalopathy.

Moreover, must be remembered the frequent presence of residual mesenchyme and liquid effusion in the middle ear cavity and mastoid cells of newborns. The mesenchyme gradually disappears in infants and children, but may persist into adulthood. (Balci et al. 2008, Sano et al. 2007). Generally, mesenchyme occupies 20% of the middle ear at birth and disappears by 1 year of age.

In middle ears with congenital anomalies, mesenchyme occupies about 30% of the middle ear at birth and does not resolve until 3 years of age (Girard et al. 1995, 800) (Figure 2).

Unfortunately, with both CT and MRI is difficult to differentiate residual mesenchyme from a simple inflammatory effusion.

Different hypotheses have been reported concerning the role of the mesenchyme in the middle ear and in the mastoid. A sort of "marrow-mesenchyme connections" may help protect the middle ear against bacterial invasion during the postnatal period. (Linthicum et al. 1997, 466-467). Conversely, other

theories hold that the connections between the hematopoietic bone marrow and middle ear could be a potential cause of childhood otogenic meningitis (Terao et al. 2011,77-80).

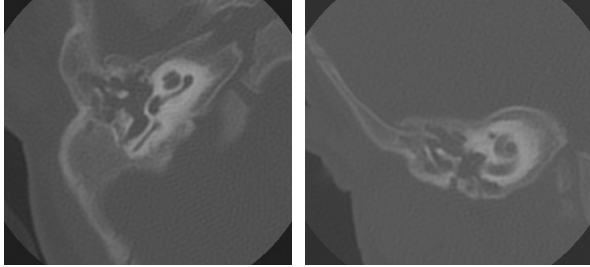


Figure 2

5-month-old male. a) Axial and b) coronal CT images. Right atresia and ossicles dysplasia. Soft tissue density inside the middle ear could be due to persistence of mesenchyme, and/or liquid effusion.

So, incidentally detected MRI abnormalities in middle ear and/or mastoid cavity of pediatric patients should be always clinically correlated in order to decide treatment requirement; empirical medical therapy is contraindicated (Balci et al. 2008, 1854).

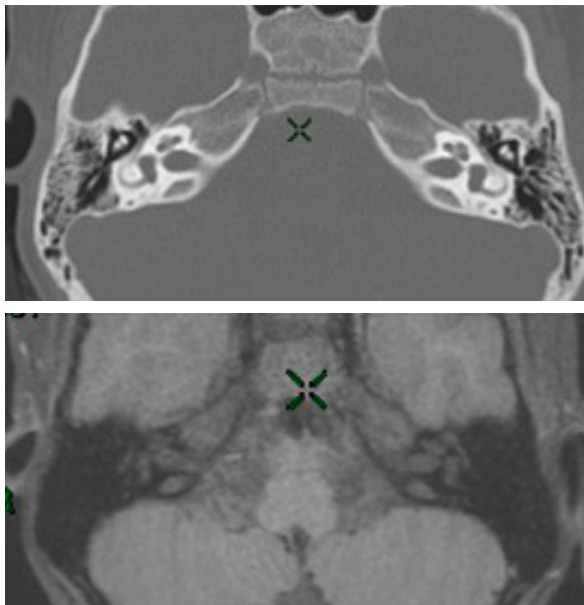


Figure 3

5-year-old male. a) Axial CT image. Middle ear and mastoid cells are bilaterally pneumatized and well aerated. b) Corresponding axial T1-weighted fat suppressed MRI image. Normal appearance of petro-mastoid cavities: compact bone and air are characterized by no signal and therefore not distinguishable from each other under normal conditions.

Generally, with increasing age, liquid effusion in the middle ear cavity disappears and the mastoid cavity develops from bone marrow to air space (Sano et al. 2007, 824) (Figure 3). However, the abnormal signal intensities on MRI should be noted in the radiological reports and newborn and infants should be examined carefully in terms of middle ear disease (Balci et al. 2008, 1853-1854).

MRI anomalies in the middle ear in older children and adults are more likely related to the presence of inflammatory pathology, often asymptomatic or paucisymptomatic. In these cases a global and accurate clinical evaluation is extremely important, with particular regard to the paranasal sinuses. The spread of MRI signal abnormalities along the Eustachian tubes, probably related to inflammation, must be reported as potentially responsible for tubal dysfunction (Figure 4).

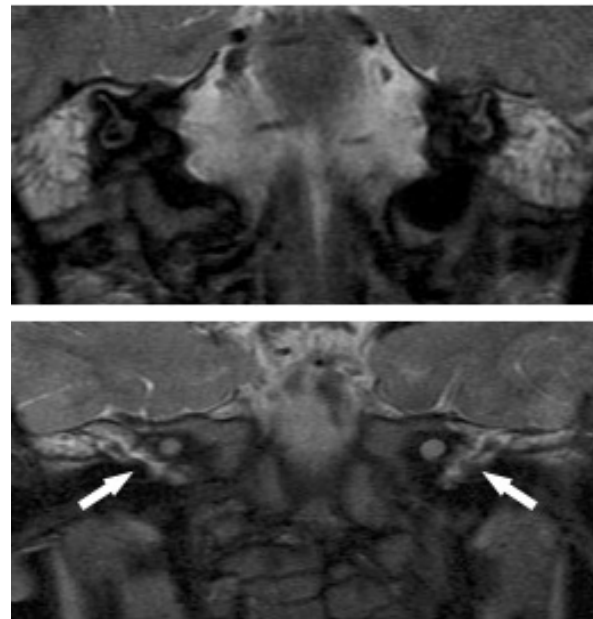


Figure 4

a-b) Coronal T2-weighted MRI images. Abnormal hyperintense signal in both mastoid regions spread along the Eustachian tube (arrows), probably related to inflammation.

1.b Ossicles

Ossification of the ossicles seems to occur steadily throughout fetal life and after birth. Bone marrow was observed in both the malleus and incus in children until 25 months of age, whilst after the age of 25 months, no bone marrow tissue was present in either of

the ossicles (Yokoyama et al. 1999). So, on CT examination performed before 25 months of age, focal hypodensities of the ossicular chain should not be misinterpreted as congenital abnormalities or acquired lesions (Figure 5).

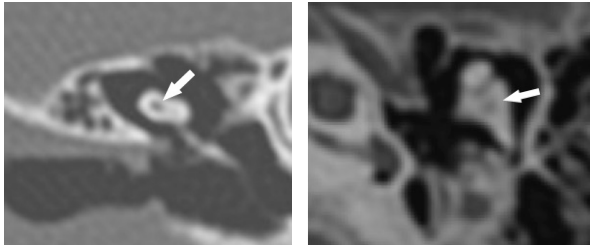


Figure 5

a) 1-year-old female, coronal CT image. b) 1-year-old male, axial CT image. Focal hypodensity due to persistence of bone marrow (arrows), respectively in the head of the malleus (a) and body of the incus (b).

About the ossicles, it should be remembered that in adulthood have been described on CT focal areas of pneumatization centered at the junction of the body and long process of the incus, and the head or manubrium (handle) of the malleus. Also these findings are presumably normal variants and the etiology is presumably developmental: it is conceivable that small gaps at the primitive marrow spaces of the incus and malleus allow for migration of mesenchyme into the ossicles, thus leaving a tiny pneumatized cavity after regression. Anyway, the pneumatized incus and malleus should be mentioned in reports, especially in cases where ossicular replacement / prosthesis is considered, because a pneumatized ossicle may be more prone to fracture (Bhatt et al. 2021).

1.c Inner ear

A sort of pericochlear hypodensity on CT is often detected in childhood. (Benson et al. 2019, 211-212; de Brito et al. 2006). On CT coronal images this so called "cochlear cleft" appears as a C-shaped lucency in the otic capsule, that extends from the cochlea to the promontory in a plane parallel to the basal turn of the cochlea (Figure 6a). On axial images usually appears as a nodular hypodensity in front of the oval window (Figure 6b).

The cochlear cleft can also be demonstrated by MRI, albeit with less evidence, as a sort of thin pericochlear canal, with an intense sig-

nal on T2-weighted images, similar to labyrinthine liquids (Figure 6c).

This finding should not be confused with pathologic entities such as otosclerosis or osteogenesis imperfecta, diseases not frequent in the pediatric population. As a consequence of the improvement of CT equipment, cochlear cleft may be seen with a prevalence ranging from 32 to 40% in pediatric patient without clinical signs suspected for otosclerosis or osteogenesis imperfecta, undergoing ear CT for other clinical reasons (Benson et al. 2019, 211-212; de Brito et al. 2006).

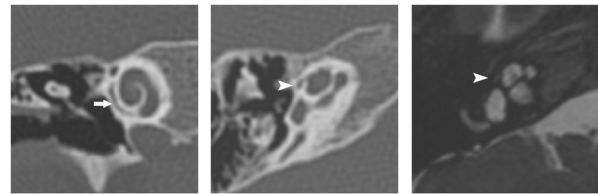


Figure 6

1-year-old female. a) Coronal CT image. "Cochlear cleft", a C-shaped lucency extended from the cochlea to the promontory (arrow). b) Axial CT image. The cochlear cleft appears as a nodular hypodensity in front of the oval window (arrowhead). c) Corresponding axial T2-weighted MRI image. The cochlear cleft has signal similar to labyrinthine liquids, but less intense (arrowhead).

The cochlear cleft may represent an extension of the fissula ante fenestram, or a remnant of petrous apex development (Benson et al. 2019, 211-212). It can be due to incomplete ossification of the otic capsule, with persistence of cartilaginous remnants (de Brito et al. 2006; Basraoui et al. 2018, 20). Therefore, caution is required in the radiological report in referring this finding to congenital malformation or labyrinthine dystrophy.

2 Otosclerosis

Otosclerosis is seldom seen in the radiological routine diagnostics due to audiological findings often being diagnostic. Radiologists detect otosclerosis findings rather more often in cases of unclear hearing loss or cochlear implant candidates. The findings may be very subtle. They require a target search and an optimal imaging technique. CT is regarded as the method of choice, widely available (Koesling et al. 2020, 745). Cone beam CT (CBCT) is a reliable method that uses a low dose of ra-

diation to investigate conductive hearing loss with intact tympanic membrane in adults. Its relevance and potential superiority to multi-detector CT in diagnosing otosclerosis remain to be demonstrated, but the preliminary data are promising (Debeaupre et al. 2019).

The otospongiotic stage of otosclerosis is characterized by areas of reduced bone density (demineralized zones) and is the easiest to detect. (Koesling et al. 2020, 747) The otic capsule just anterior to the oval window is the typical site of manifestation (Figure 7).

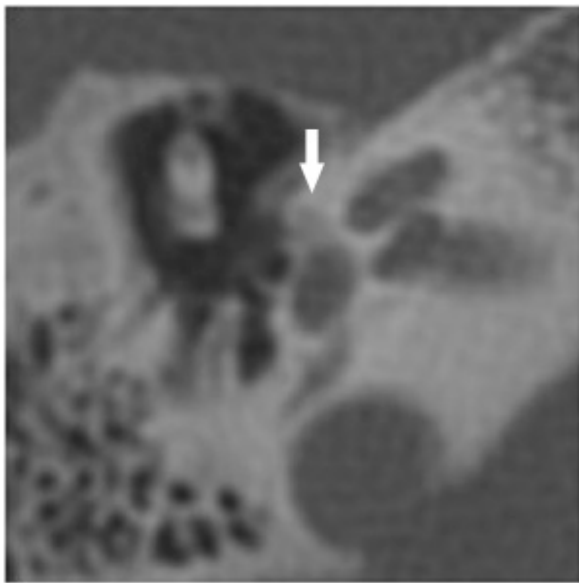


Figure 7

50-year-old female. Axial CT image. Otospongiotic stage of otosclerosis: area of reduced bone density just anterior to the oval window (arrow).

Disease limited to this area is referred to as fenestral otosclerosis and is most commonly lucent on CT due to resorption of the enchondral bone during the spongiotic (active) phase. (Sanghan et al. 2018, 2350).

Less frequent are demineralized zones on the promontory, the round window (RW) and the tympanic facial canal. Very small foci of CT hypodensity are often overlooked in routine diagnostics, not least due to a suboptimal examination technique (Koesling et al. 2020, 747)). The involvement of the RW occurs in 30% of clinical cases (Mansour et al. 2011, 384). This structure must still be carefully evaluated by radiologist, also keeping in mind his possible isolated involvement (Figure 8). The extension of retrofenestral otosclerosis to the RW may preclude a good surgical out-

come, even after successful stapedectomy (Bae, 2019, 1191).

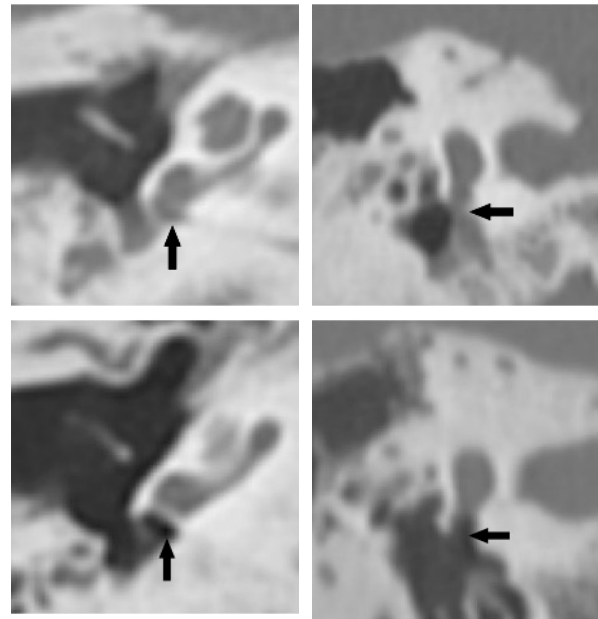


Figure 8

a-b) 47-year-old male. Axial and coronal CT images. Otospongiotic tissue fills the round window (arrows). c-d) Normal case, axial and coronal CT images. Round window well aerated (arrows).

In more striking cases, bone rarefaction caused by otospongiosis can be very widespread, and therefore easily detected by CT (Figure 9).

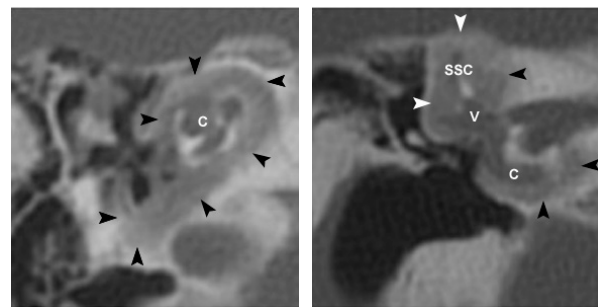


Figure 9

39-year-old female with otosclerosis. a) Axial and b) coronal CT images. Large and widespread area of bone rarefaction caused by otospongiosis (arrowheads). Cochlea (c), vestibule (v), superior semicircular canal (ssc).

Moreover, in case of clinical suspect of otosclerosis, detect the only finding of a relatively hypodense stapes compared to the remaining portion of the ossicular chain can generate interpretative doubts (Figure 10).

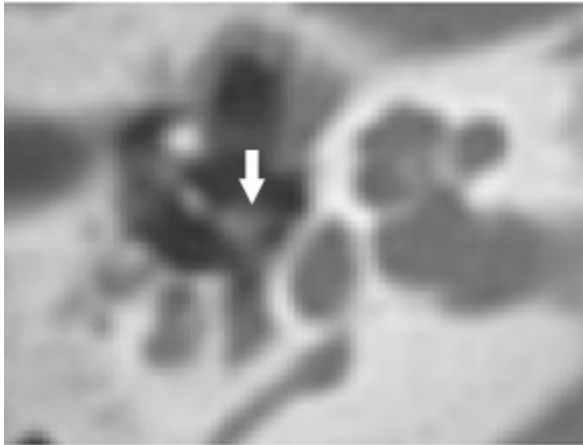


Figure 10
47-year-old male with clinical symptoms of otosclerosis. Axial CT image. Relatively hypodense stapes (arrow) compared to the remaining portion of the ossicles could be caused by otospongiosis.

Histologic alterations in the superstructure of the stapes have however been described in patients operated for otosclerosis (Carvalho et al. 2015). Thus, stapes hypodensity could be a sign of otosclerosis.

As the disease progresses to the inactive or sclerotic phase when remodeling processes are suspended, these lesions undergo remineralization, become more dense and difficult to differentiate from normal surrounding bone (Koesling et al. 2020, 747; Sanghan et al. 2018, 2350).

On MRI the diagnosis of otosclerosis is difficult or impossible. A false negative result is usually obtained in routine examinations. Anyway, during the active phase, the otospongiotic foci may accumulate contrast agent, which is only noticeable on thin-sliced (≤ 2 mm) T1-weighted or FLAIR sequences. In the sclerotic stage, the diagnosis cannot be made by MRI (Koesling et al. 2020, 748-749).

3 Arteries

Anomalies of the intrapetrosal tract of the internal carotid artery (ICA) are well known: absent (Ottaviano et al. 2007), aberrant or duplicated ICA have been widely described (Roll et al. 2003; Anagiotos et al. 2019; Calzolari, Martini 2009,115). Anyway, in addition to any carotid anomalies, the radiologist should be reminded of the importance of reporting al-

ways the distance between carotid and cochlea before implant surgery.

3a Persistent stapedia artery

A persistent stapedia artery (PSA) is a not frequent vascular anomaly with a prevalence calculated to be 0.48% in a histopathologic study of 1000 temporal bones. This vascular anomaly can be isolated or associated with other middle ear abnormalities, most commonly involving the stapes, facial nerve, or ICA; it may also be present in trisomy 13, 15, and 21, as well as in Paget's disease, otosclerosis, thalidomide deformities, anencephaly, congenital immunodeficiency, and neurofibromatosis. A PSA can cause conductive hearing loss and has been described as a cause of pulsatile tinnitus (Thiers et al. 2000). The PSA appears on CT as a small vascular structure leaving the carotid canal and passing through the stapes to join the facial nerve canal (Figure 11). Other CT findings of this anomaly are an enlarged facial nerve canal or a separate canal parallel to the facial nerve, and the absence of the foramen spinosum, because the PSA becomes the middle meningeal artery by entering the tympanic cavity through the facial hiatus. (Thiers et al. 2000; Koesling et al. 2005, 341). The precise report of PSA is mandatory, especially before middle ear and cochlear implant surgery.

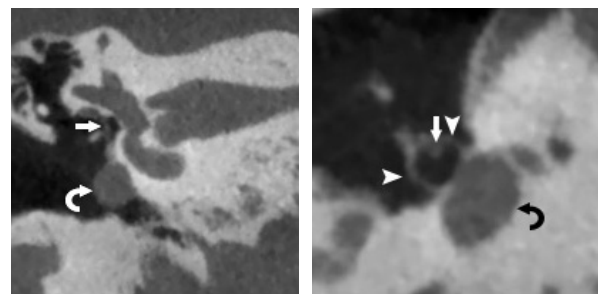


Figure 11
28-year-old female with occasional throbbing sensation in the right ear and transient tinnitus. a) Coronal CT image. Right persistent stapedia artery runs in the middle ear in front of the oval window (arrow); aberrant right carotid artery (curved arrow). b) Oblique reformatted CT image. The stapedia artery (arrow) passes through the crura of the stapes (arrowheads); vestibule (curved arrow). Courtesy of Dr. L. Pinelli, Neuroradiology Department, Spedali Civili, Brescia, Italy

3b Subarcuate artery

The subarcuate artery (SAA) is a very thin vessel that originates from the anterior inferior cerebellar artery in 80% of cases, from an accessory anterior inferior cerebellar artery in 17%, from the posterior inferior cerebellar artery in 3% and only in a few cases from the internal auditory artery. The SAA provides blood supply to the bony labyrinth, the facial canal and the mastoid antrum. In its intrapetrous course, the artery runs inside the subarcuate canal (SAC), divided into three segments: proximal, intermediate and distal (Grammatica et al. 2010). In the proximal segment, the SAC enters into the posterior aspect of the petrous bone (Figure 12).

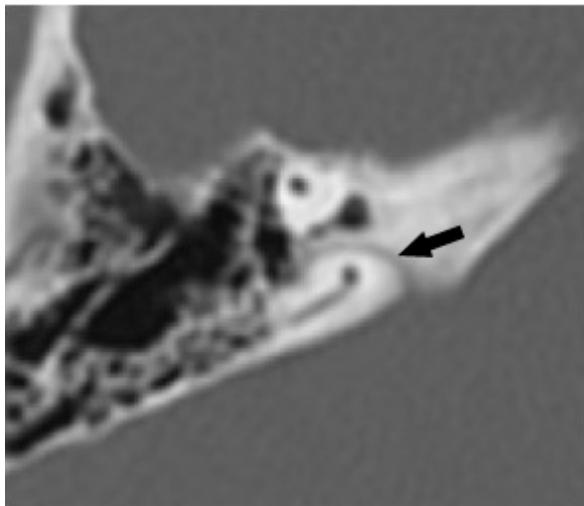


Figure 12
10-year-old female. Axial CT image. Right subarcuate artery: the proximal segment of the subarcuate canal enters into the posterior aspect of the petrous bone (arrow).

The intermediate tract runs deeply in the petrous bone and reaches the superior semicircular canal passing under its arch; the distal segment runs to the antrum where it stops (Figure 13). Normally the SAC is 1 mm in width, but cases wider are described (Grammatica et al. 2010, Tekdemir et al. 1999). The SAC course is not always constant and several variations are described, both in anatomical dissection and CT studies. This condition may have important consequences in some otologic approaches, especially in the retrofacial approach during tympanoplasty (Grammatica et al. 2010, 173). Moreover, the presence of dura mater tissue and also of a vein along

the course of the canal makes it a potential route for infectious spread from the mastoid air cells (Benson et al. 2020, 211). Fractures that cross the course of the canal can have effects on the blood supply of the labyrinth and related symptoms.

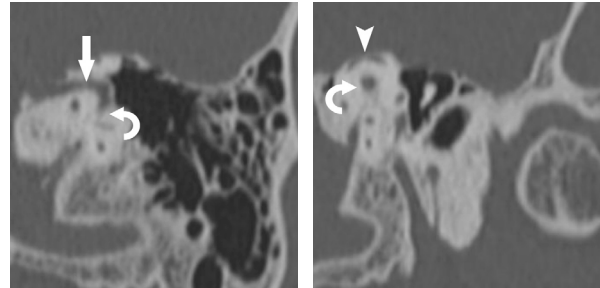


Figure 13
65-year-old male. Left subarcuate artery and canal. a) Oblique reformatted CT image, parallel to intermediate segment of the subarcuate canal (arrow); knee between intermediate and distal segment of the canal (curved arrow). b) Oblique reformatted CT image, perpendicular to intermediate segment of the subarcuate canal (curved arrow); superior semicircular canal (arrowhead).

4 Veins and other

4a Internal jugular vein

Usually there is caliber asymmetry between left and right internal jugular vein (IJV). Amongst the venous anomalies, a large and/or high jugular bulb (JB) is undoubtedly the most frequent; a high JB has influence on the approach in acoustic neurinoma surgery (Koesling et al. 2005, 342). Dilation of the jugular vein and its eventual tympanic dehiscence may coexist (Figure 14); if the dilated vein protrudes into the middle ear it can be confused with a glomus tumor by otoscopy. These anatomical variations must be described on imaging performed before surgery; in particular, they must be excluded by CT before a "full ear" myringotomy and may influence the choice of the side for cochlear implantation.

4b Internal jugular vein and endolymphatic sac

The JB dilation should not be confused with a dilation of the endolymphatic sac (ES), an anomalous structure in correspondence with the posterior surface of the petrous bone. The

dilation of the ES and of the endolymphatic duct (ED) may occur isolated or associated and represents the anatomic-pathological substrate of the so called "enlarged vestibular aqueduct" (EVA) syndrome.

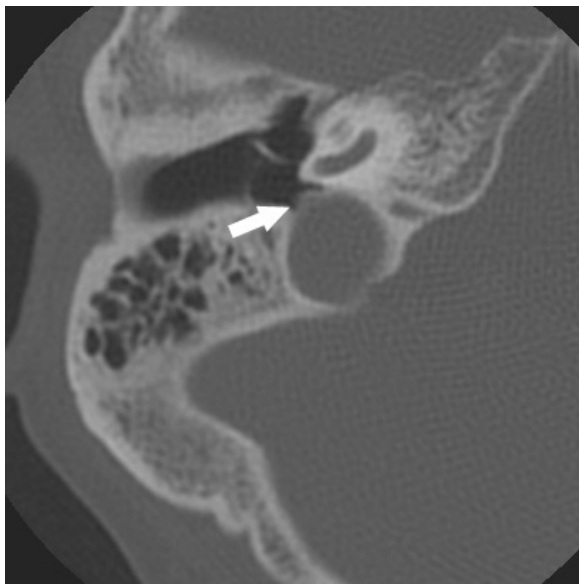


Figure 14

Axial CT image. Tympanic dehiscence of a large jugular vein (arrow).

This syndrome is characterized by a clinical picture of highly variable hearing loss; it should be included in the differential diagnosis of unexplained mixed hearing loss (Santos et al. 2010). The ED and the ES are the not sensory components of the endolymph-filled, closed, membranous labyrinth. The ED runs from the utricular and saccular ducts within the vestibule through the vestibular aqueduct (VA) to the ES, which extends through the distal VA out the external aperture of the aqueduct to terminate in the epidural space of the posterior cranial fossa (Lo et al. 1997).

The vestibular aqueduct is considered enlarged when its anterior-posterior diameter or lateral-medial dimension, measured at its mid-portion, is 1.5 mm or greater (Calzolari, Martini 2009, 110). Dilation of VA, a bone canal, is well demonstrated by CT (Figure 15a); dilation of both ES and ED is visible on MRI T2-weighted images (Figure 15b). So, the syndrome may be misrecognized by CT if only dilation of the extracanal portion of the ES occurs, without dilation of the ED and consequently of the VA. There is also the possibility of exclusive dilation of the duct, visible both

in CT and in MRI, but not of the sac (Figure 16).

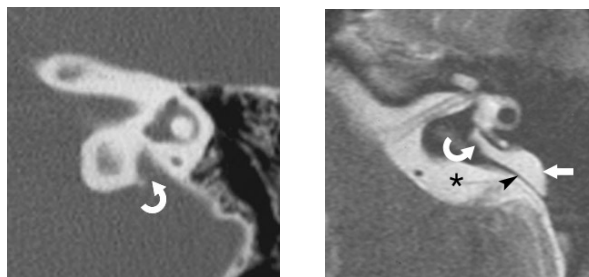


Figure 15

a) Axial CT image. Dilation of the vestibular aqueduct (curved arrow). b) Corresponding axial T2-weighted MRI image. Dilation of the endolymphatic duct (curved arrow) and sac (arrow); dura mater (arrowhead), subarachnoid space (asterisk).

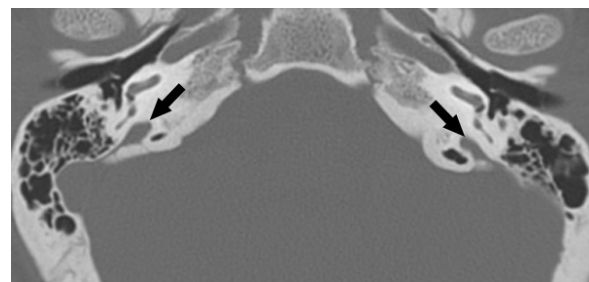


Figure 16

a) Axial CT image. Bilateral dilation of the vestibular aqueduct (arrows). b) Corresponding axial T2-weighted MRI image. Dilation of both endolymphatic ducts (arrows), but not of the sacs; subarachnoid spaces (asterisks).

Dehiscence between a high JB and the ES was demonstrated in temporal specimens. In particular, a bony dehiscence was localized on the lateral ES and only connective tissue was present in that area between the ES and the JB. Because in these cases neither endolymphatic hydrops nor audiological symptoms were found, the possibility that a high JB affects function in the inner ear remains to be studied (Kawano et al. 2000, 168).

In the author's experience a strange case of ambiguous differentiation between a high JB and a large but thin ES was found. Thanks to the different technical characteristics of the acquired images, CT and MRI findings proved without a doubt a close contact between a wide but thin ES that hooded a large, high and lateral JB (Figure 17). In this anatomical situation, it is hypothesized the venous pulsations can be transmitted to the endolymphatic sac; it could cause aberrant transmitted signals to the vestibular and cochlear nerve, producing dizziness or hearing loss.

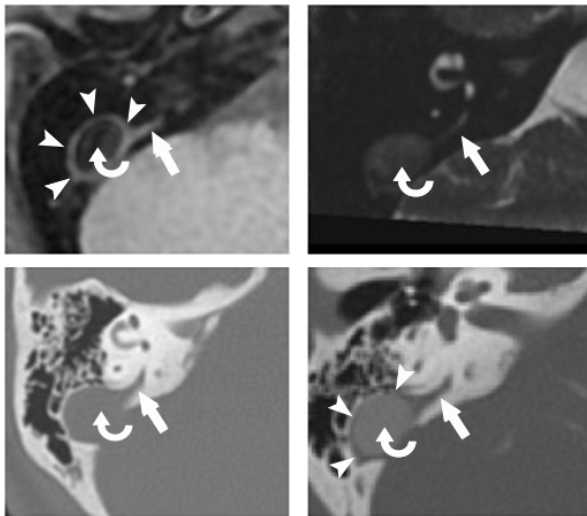


Figure 17

11-year-old female. Dehiscence between a high jugular bulb and the endolymphatic sac. a) Axial T1-weighted fat suppressed MRI image. Endolymphatic duct (arrow); thin endolymphatic sac (arrowheads) surrounding the jugular bulb (curved arrow). The duct and the sac have the same intermediate signal; the jugular bulb has a lower and inhomogeneous signal, due to turbulence of the venous flow. b) Axial T2-weighted MRI image. Endolymphatic duct (arrow); the endolymphatic sac and the jugular bulb are indistinguishable from each other (curved arrow). c) Axial CT image. Vestibular aqueduct (arrow); jugular fossa (curved arrow). d) Axial CT image after intravenous injection of contrast medium. The contrast medium fills the jugular bulb (curved arrow), but not the sac (arrowheads) and duct (arrow).

4c Petrosquamous sinus

The petrosquamous sinus (PSS) is an embryonic venous remnant, which usually regresses during fetal life, but occasionally per-

sists into adulthood. It is an emissary vein of the posterior fossa connecting the sigmoid or transverse sinus with the extracranial venous system. The PSS runs through the supero-lateral portion of the petrous bone; so, its anatomic course may lead to problematic bleeding during mastoidectomy and in general surgery of the skull base or middle and inner ear (Marsot-Dupuch et al. 2001, Shim et al. 2014). CT techniques of multiplanar reformatting reconstructions can be very useful in representing the course of the intrapetrous bone canal that contains the PSS (Bozek et al. 2016). On the other hand both CT and MRI must be integrated in confirming the venous nature of this finding and excluding other diagnostic possibilities (Figure 18).

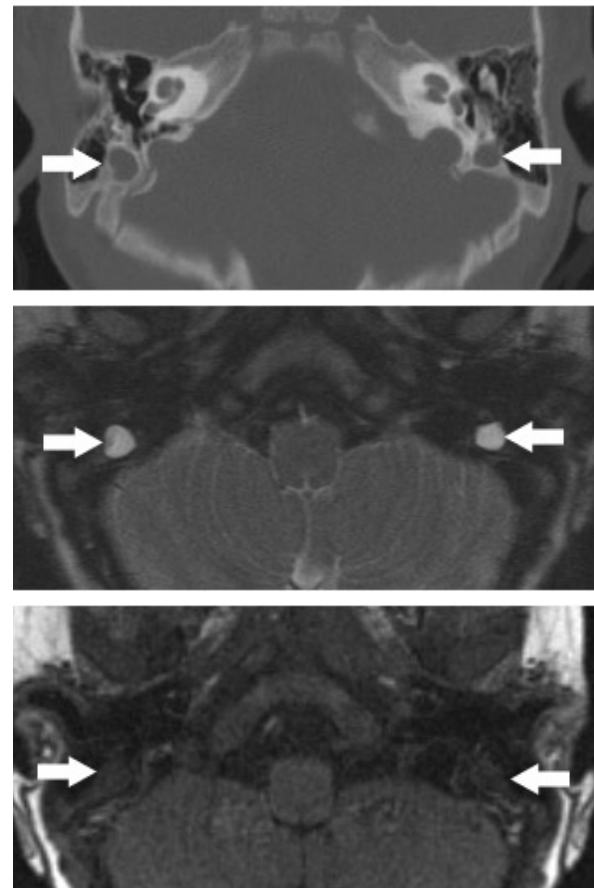


Figure 18

1-year-old male. Suspected petrosquamous sinus in cochlear implant candidate. a) Axial CT image. b-c) Corresponding axial T2 and T1-weighted contrast enhanced MRI images. The diagnosis of venous remnant was not confirmed by surgical exploration from the implant side, which showed a fluid-filled cavity, lined with fibrous tissue (arrows).

4d Mastoid emissary vein

The emissary veins cross completely the skull making a direct connection between the superficial veins of the scalp and dural sinuses. These vessels have no valves and the blood can flow in both directions, but generally from outside to inside (Kim et al. 2021, 86). The mastoid emissary vein (MEV) is an emissary vein which courses between the sigmoid sinus and sub-occipital venous plexus; it is commonly asymmetric developed (Koesling et al. 2005, 342; Sarioglu et al. 2019, 126).

Both MEV and the IJV are a part of extracranial venous drainage. When the standard conditions of venous drainage occur, the role of the MEV is limited. Conversely, it can be the main flow route in patients whose venous drainage is altered, such as in patients with high-flow vascular malformations, intracranial hypertension, or occlusion of the IJV. In this case the MEV takes on an important compensatory meaning (Kim et al. 2021, 86; Koesling et al. 2005, 342). The MEV is very well visualized on CT, especially if large; it should not be confused with the lambdoid suture, located in proximity (Figure 19). Its visibility on MRI, even if dilated, depends on its course, more or less tortuous, and flow, fast or turbulent.

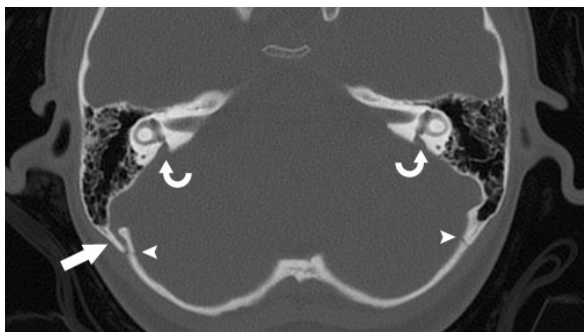


Figure 19
Axial CT image. Right mastoid emissary vein (arrow); lambdoid sutures (arrowheads). Bilateral dilation of the vestibular aqueduct (curved arrows).

Recently has been reported an unusual case of a patient with unilateral pulsatile tinnitus caused by a large, prominent mastoid emissary vein (MEV). The patient's symptoms had improved after surgical ligation (Kim et al. 2021).

The MEV is important from the neurosurgical point of view, because it can become a source of significant bleeding in surgical ap-

proaches through the mastoid process, especially in retrosigmoid craniotomy, which is used for approaches to pathologies of the cerebellopontine angle (Hampl et al. 2018). Finally, The MEVs were found more common in the CI candidates when compared to the control group (Sarioglu et al. 2019, 126). So, it should be remembered that a large MEV can hinder the intrathecal positioning of the external component of cochlear implants and therefore can influence the choice of the side; this represents a further reason why the radiologist must know this anatomical structure, identify it in the images and describe it in the report.

5 Facial nerve

Many abnormalities of the facial nerve canal in the petrous temporal bone have been documented, isolated or in association with anomaly of the external, middle and inner ear (Calzolari 2006, 333-334; Calzolari, Martini 2009, 102-103; Sennaroglu, Tahir 2020). A recent classification distinguishes the anomalies in relation to the affected segment of the nerve, i. e. meatal, labyrinthine, tympanic, and mastoid (Sennaroglu, Tahir 2020). Pre-operative radiological identification of facial nerve anomalies can help prevent intra-operative facial nerve injury, in particular during middle ear surgery, mastoidectomy and cochlear implantation (Ozaki et al. 2020, Palabiyik et al. 2017).

The most common anomaly is congenital bony dehiscence of the canal that occurs in up to 55% of otherwise normal temporal bones, predominantly involving the tympanic portion in 91% of cases (Glastonbury et al. 2003, 1335).

Facial nerve canal dehiscence is thought not to be a congenital anomaly but rather a developmental arrest of the bone canal, that should be completed at the age of 4 years; middle ear inflammation in young children could affect the development of the canal (Nomiya et al. 2014, 458). Micro and macro tympanic dehiscences may occur, 56% and 69%, respectively (Gulotta et al. 2020, 367).

The nerve can protrude into the tympanic cavity, more or less covered by a bone wall of variable thickness (Figure 20), or run completely free in the cavity, without bone covering (Figure 21). The tympanic dehiscence,

well visualized on CT, must be absolutely described by the radiologist, as it is potentially dangerous not only in the case of surgery, but also for a lesser protection of the nerve when intratympanic pathology occurs.

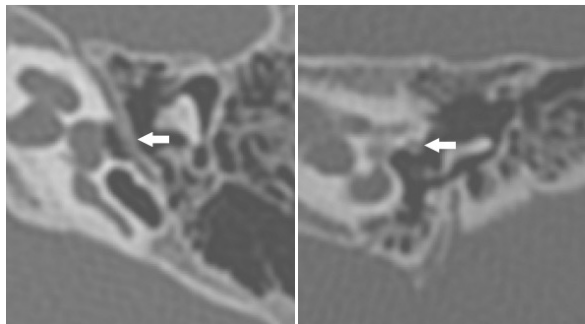


Figure 20
a) Axial and b) coronal CT images. Tympanic dehiscence of the left facial nerve. Only the upper half of the intratympanic tract of the nerve is covered by a bony hemi-canal (arrows).

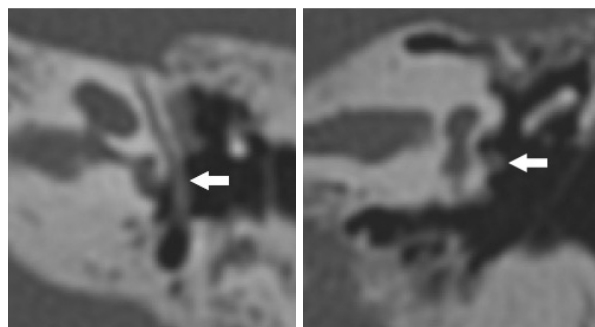


Figure 21
13-year-old male. a) Axial and b) coronal CT images. Tympanic dehiscence of the left facial nerve. The nerve runs completely free in the cavity, without bone covering (arrows).

Rarer is the dehiscence of the mastoid segment of the facial nerve into the jugular fossa, generally in association with a wide JB. In this case the nerve is in direct contact with a huge vein (Figure 22). Recurrent facial weakness has been described as a consequence, precipitated by visiting places of high altitudes, which may have increase the dilatation of the jugular bulb (Alkhamis et al. 2021). Irritation of the dehiscent facial nerve in the jugular fossa could occur whenever venous pressure increases, for instance with the Valsalva maneuver. Also, venous catheterization used for blood gas analysis or in angiographic procedures could cause microtrauma to the facial nerve closely in contact with the jugular vein.

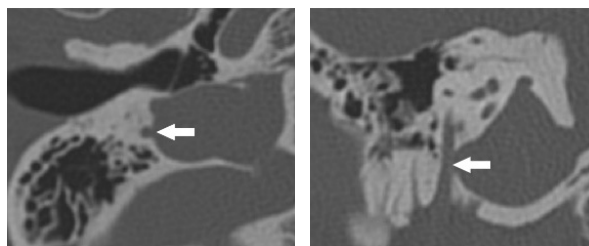


Figure 22
42-year-old female. a) Axial and b) coronal CT images. Dehiscence of the mastoid segment of the right facial nerve into the jugular fossa, in contact with a wide jugular bulb (arrows).

Concerning the mastoid segment of the facial nerve, well known is the occurrence of anterior dislocation in case of atresia and middle ear malformations (Calzolari 2006, 333-334; Calzolari, Martini 2009, 103) (Figure 23).

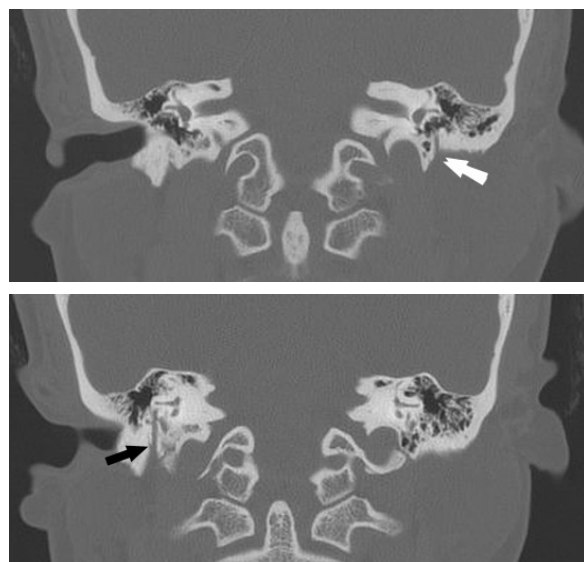


Figure 23
20-year-old female. Coronal CT images. Left microtia and atresia. a) Anterior dislocation of the mastoid segment of the left facial nerve (arrow). b) Normal situation of the right nerve (arrow).

Finally, duplication of the facial nerve is a very rare anomaly commonly associated with middle and inner ear anomalies. It can involve any segment of intratemporal facial nerve, but there are few isolated case reports describing bifurcation of mastoid segment (Glanstonbury et al. 2007; Jakkani et al. 2013).

The duplication may be found on both side (Figure 24). The detection of this anomaly is important in presurgical evaluation to avoid inadvertent nerve injury and as well as to di-

rect the radiologist to look for the presence of other congenital anomalies (Glanstonbury et al. 2007; Jakkani et al. 2013).

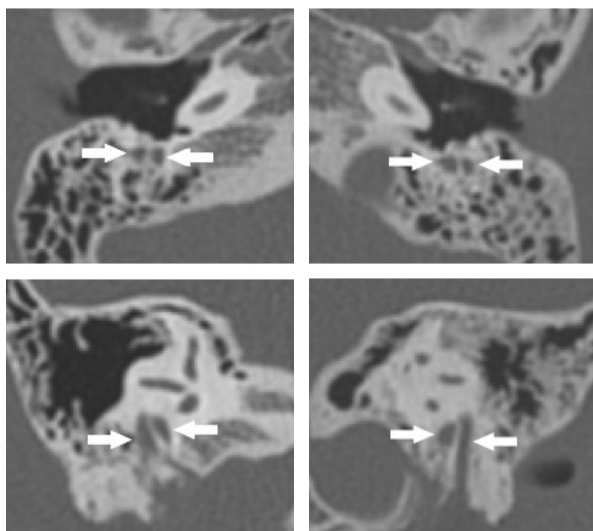


Figure 24
6-year-old male. a-b) Axial and c-d) coronal CT images. Duplication of the mastoid segment of the facial nerve on both side (arrows).

6 “Pseudofractures”: fissures (sutures) and other canals.

Thanks to high resolution images and thin section, a lot of temporal fissures and bone channels may be visualized on routine CT imaging. In patients studied for head trauma normal fissures (or sutures) and channels can lead to the pitfall of being interpreted as “fractures”, so much so that they are called “pseudofractures” (Kwong et al. 2012, 428; Koesling et al. 2005, 339). Temporal bone pseudofractures can be divided into three categories: intrinsic fissures, which are formed between the five parts of the temporal bone; extrinsic fissures, which are formed by the borders of the temporal bone with the rest of the skull; and intrinsic canals, in which various structures, such as arteries, veins, nerves and inner ear ducts run (Kwong 2012, 428).

6a Fissures.

The intrinsic fissures are tympanosquamous, petrotympanic (Figure 25), petrosquamous and tympanomastoid sutures (Kwong et al. 2012, 428). The extrinsic fissures are occipitomastoid, petrooccipital (Figure 25), sphenosquamosal and sphenopetrosal sutures (Kwong et al. 2012, 428-429).



Figure 25
26-year-old female. Axial CT image. Intrinsic fissures: tympanosquamous (arrow), petrotympanic (arrowhead). Extrinsic fissure: occipitomastoid (curved arrow), petrooccipital (angled arrow). The sutures, in particular the extrinsic ones, have a non-linear or knurled course, with a rim characterized by margins of compact cortical bone. Mandibular condyle (short arrow), glenoid cavity (asterisk).

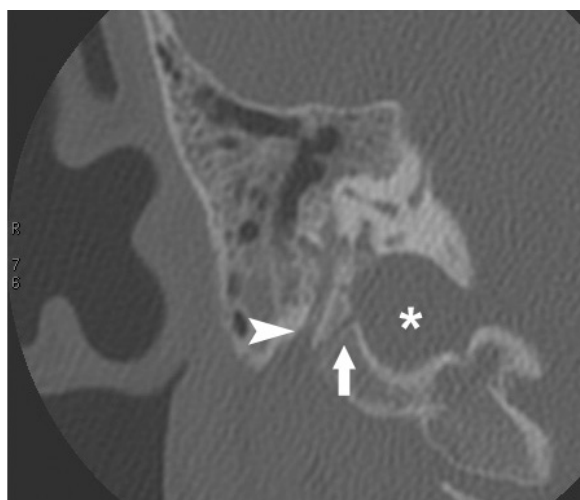


Figure 26
Coronal CT image. Temporal fracture interesting the lateral wall of the jugular fossa (arrow). The fracture line is not delimited by compact bone, but by spongy bone. This fracture is potentially dangerous for damage to the facial nerve (arrowhead) and the jugular bulb (asterisk).

The visibility of sutures depends on their size and the imaging parameters; the best visibility occurs on images with the smallest slice thickness (1.5 mm) and with newborns as patients. With increasing age the gap be-

tween the bones is diminishing and the cranial bones are toothed; complete closure was observed until the seventh decade (Koesling et al. 2005, 340). The sutures, in particular the extrinsic ones, have a non-linear or knurled course, with a rim characterized by margins of compact cortical bone (Figure 25), while in general the fractures are more linear, and the discontinuity is not delimited by compact bone (Figure 26).

6b Intrinsic canals

Among the intrinsic canals, in addition to those described above (SAC, VA, facial canal) some others can be remembered.

The inferior tympanic canaliculus contains the tympanic nerve (nerve of Jacobson), a branch of the glossopharyngeal nerve, which arises from the petrous ganglion, and ascends to the tympanic cavity (Figure 27). The inferior tympanic artery also runs through. In case of aberrant ICA with absent petrous ICA, the inferior tympanic artery enlarges to form the proximal cranial ICA (Kwong et al. 2012, 429). Multiplanar CT imaging is useful to demonstrate this canal (Mazziotti et al. 2011).

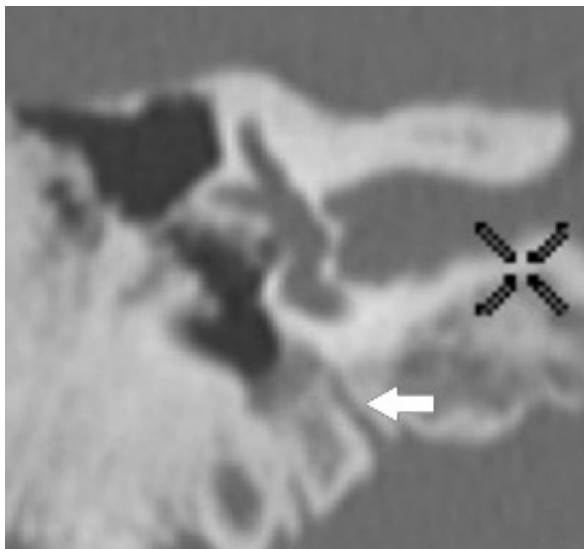


Figure 27
47-year-old male. Coronal CT image. Inferior tympanic canaliculus (arrow), which contains the tympanic nerve (nerve of Jacobson).

The cochlear aqueduct connects the subarachnoid space to the scala tympani of the cochlea basal turn, close to the round window. CT studies have demonstrated it to be

12.3 mm in length; its external medial aperture is funnel-shaped (Figure 28). Functionally, the cochlear aqueduct likely plays a role in maintaining a pressure balance between the cerebrospinal fluid (CSF) and inner ear. Within the aqueduct are connective tissue, fibroblasts, and sometimes a patent central lumen making up the perilymphatic duct, but there is controversy as to the patency of this duct in adults (Kwong et al. 2012, 429; Benson et al. 2020, 210-211).

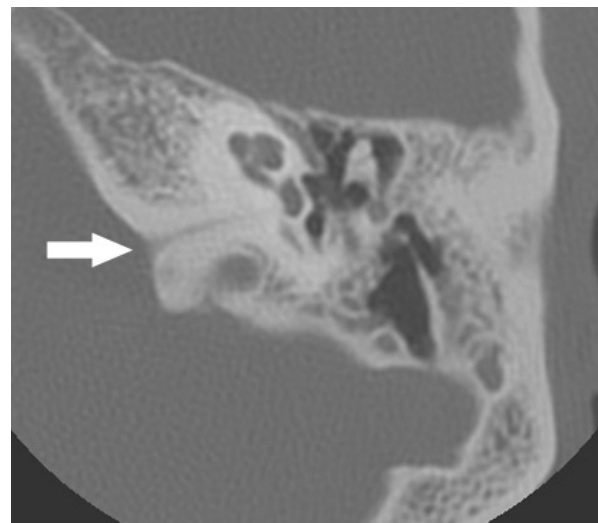


Figure 28
Axial CT image. Cochlear aqueduct, with funnel-shaped medial aperture (arrow).

The singular canal extends from the posterior margin of the internal auditory canal (IAC) to the posterior semicircular canal; this finding can be bilateral (Figure 29). Through the canal runs the posterior ampullary nerve (also known as the singular nerve), which branches from the inferior vestibular nerve and transmits afferent signals from the ampulla of the posterior semicircular canal. The singular canal is rarely of radiologic importance, although it may be confused for an acute fracture (Benson et al. 2020, 211). However, the singular canal is an important landmark during a retrosigmoid approach to vestibular schwannomas because its identification prevents accidental labyrinthine damage (Kwong et al. 2012, 429). Moreover, it is the target of singular neurectomy, a treatment option for refractory benign paroxysmal positional vertigo (Benson et al. 2020, 211).



Figure 29
9-year-old female. Axial CT image. Bilateral singular canal, extended from the posterior margin of the internal auditory canal to the vestibule (arrows). Through the canal runs the posterior ampullary nerve, also known as the singular nerve.

Conclusion

CT and MRI are integrated in the diagnostic imaging of the ear and the temporal bone, albeit considering the specificity of CT in the morphological and detailed demonstration of bone structures and the peculiarity of MRI in characterizing pathological tissue.

Modern equipment makes it possible to represent normal or pathological structures even of small dimensions and therefore not immediately perceptible to the observer of the images.

However, to fully exploit the potential of both CT and MRI it is necessary not only to have adequate equipment, but also to use standardized diagnostic protocols consistent with the clinical question, and carry out the investigations with the correct technique.

References

- Alkhamis, F., Alhajri, K., Aljaafari, D., Alhashim, A., Alsamarah, A., Sharydah, A., Basheir, O., Al Sulaiman, F., Alabdali, M. (2021) Recurrent facial palsy due to high jugular bulb dehiscence, *J Multidiscip Healthc*, 14, 359-362.
- Anagiotos, A., Kazantzi, M., Tapis, M. (2019) Aberrant internal carotid artery in the middle ear: the duplication variant, *BMJ Case Rep*, 12 (4), e228865.
- Bae, Y. J., Shim, Y. J., Choi, B. S., Kim, J. H., Koo, J. W., Song, J. J. (2019) "Third window" and "single window" effects impede surgical success: analysis of retrofenestral otosclerosis involving the internal auditory canal or round window, *J Clin Med*, 8 (8), 1182-1193.
- Balci, A., Sangun, O., Okuyucu, S., Karazincir, S., Akoglu, E., Altintas, Y., Egilmez, E. (2008) The prevalence and significance of incidental middle ear and mastoid cavity abnormalities on MRI in a pediatric population, *Int J Pediatr Otorhinolaryngol*, 72 (12), 1849-1854.
- Basraoui, D., Elatiqi, K., Jalal, H. (2018) Computed tomography of the petrous bone: particularities in children, *Advances in Molecular Imaging*, 8, 15-24.
- Benson, J.C., Eckel, L., Guerin, J., Silvera, V. M., Diehn, F., Passe, T., Carlson, M. L., Lane, J. I. (2020) Review of temporal bone microanatomy: aqueducts, canals, clefts and nerves, *Clin Neuroradiol*, 30 (2), 209-219.
- Bhatt, A .A., Desai, A., Sandhu, S. J. S., Vibhute, P. (2021) Pneumatized middle ear ossicle - A normal variant, *Clin Imaging*, 69, 179-181.

Considering the now widespread accessibility to the most modern imaging technologies, it is still mandatory to use the investigations appropriately, in relation to clinical suspect, therapeutic needs and compliance with the cost / benefit ratio.

It is also necessary to respect the concept of always using the method and technique less invasive for the patient, safeguarding the radiation protection criteria, especially in the pediatric age.

Finally, regarding temporal and ear imaging (but not only!) the knowledge of the anatomy, anatomic variants and of up-to-date embryological concepts enables the production of a radiological report, which is not only descriptive but also interpretative, suggesting clinical correlations, surgical cautions, further investigations or genetic counselling. A precise and detailed report helps to avoid misinterpretation as pathological lesions and iatrogenic complications, in particular intra-operative bleedings which could be very serious or even fatal.

The dialogue and collaboration between the radiologist and the audiologist remains fundamental to direct and carry out the diagnostic activity in the interest and safety of the patient and to contain costs for the population.

- Bożek, P., Kluczevska, E., Misiołek, M., Ścierański, W., Lisowska, G. (2016) The prevalence of persistent petrosquamosal sinus and other temporal bone anatomical variations on high-resolution temporal bone computed tomography, *Med Sci Monit*, 4 (22), 4177-4185.
- Calzolari, F. (2006) Diagnostica per immagini delle malformazioni congenite dell' orecchio esterno e dell' orecchio medio, in Martini, A. (ed.), *Genetica della funzione uditiva normale e patologica*, Torino, Italy: Omega Edizioni, 323-343.
- Calzolari, F., Martini, A. (2009) Radiological abnormalities of the ear, in Newton, V. E. (ed.), *Paediatric audiological medicine*, Chichester, United Kingdom: Wiley-Blackwell, 90-125.
- Carvalho, B., Hamerschmidt, R., Telles, J. E., Richter, N. (2015) Anatomopathology of the superstructure of the stapes in patients with otosclerosis, *Int Arch Otorhinolaryngol*, 19, 1-4.
- Debeaupre, M., Hermann, R., Pialat, J. B., Martinon, A., Truy, E., Ltaief Boudrigua A. (2019) Cone beam versus multi-detector computed tomography for detecting hearing loss, *Eur Arch Otorhinolaryngol*, 276 (2), 315-321.
- de Brito, P., Metais, J. P., Lescanne, E., Boscq, M., Sirinelli, D. (2006) Hypodensité tomographique péricochléaire: variante de la normale chez l'enfant, *J Radiol*, 87 (6 Pt 1), 655-659.
- Girard, N., Raybaud, C., Locatelli, P., Magnan, J. (1995) Ear malformations, *Rivista di Neuroradiologia*, 8 (6), 793-814.
- Glastonbury, C. M., Fischbein, N. J., Harnsberger, H. R., Dillon, W. P., Kertesz, T. R. (2003) Congenital bifurcation of the intratemporal facial nerve, *Am J Neuroradiol*, 24 (7), 1334-1337.
- Grammatica, A., Alicandri-Ciuffelli, M., Molteni, G., Marchioni, D., Presutti, L. (2010) Subarcuate canal and artery: a case report, *Surg Radiol Anat*, 32 (2), 171-174.
- Gulotta, G., Pace, A., Iannella, G., Visconti, I. C. (2020) Facial nerve dehiscence and cholesteatoma: a comparison between decades, *J Int Adv Otol*, 16(3), 367-372.
- HAMPL, M., Kachlik, D., Kikalova, K., Riemer, R., Halaj, M., Novak, V., Stejskal, P., Vaverka, M., Hrabalek, L., Krahulik, D., Nanka, O. (2018) Mastoid foramen, mastoid emissary vein and clinical implications in neurosurgery, *Acta Neurochir*, 160 (7), 1473-1482.
- Isaacson, B. (2018) Anatomy and surgical approach of the ear and temporal bone, *Head Neck Pathol*, 12 (3), 321-327.
- Jakkani, R. K., Ragavendra, K. I., Karnawat, A., Vittal, R., Kumar, A. D. (2013) Congenital duplication of mastoid segment of facial nerve: a rare case report, *Indian J Radiol Imaging*, 23, 35-37.
- Kawano, H., Tono, T., Schachern, P. A., Paparella, M. M., Komune, S. (2000) Petrous high jugular bulb: a histological study, *Am J Otolaryngol*, 21 (3), 161-168.
- Kim, S. G., Koh, J. H., Kim, B. J., Lee, E. J. (2021) Surgical ligation of a large mastoid emissary vein in a patient complaining of pulsatile tinnitus, *J Int Adv Otol*, 17 (1), 84-86.
- Koesling, S., Kunkel, P., Schul, T. (2005) Vascular anomalies, sutures and small canals of the temporal bone on axial CT, *Eur J Radiol*, 54 (3), 335-343.
- Koesling, S., Plontke, S. K., Bartel, S. (2020) Imaging of otosclerosis. *Rofo*, 192 (8), 745-753.
- Kwong, Y., Yu, D., Shah, J. (2012) Fracture mimics on temporal bone CT: a guide for the radiologist, *Am J Roentgenol*, 199 (2), 428-434.
- Linthicum, F. H, Jr, Tian, Q., Slattery, W. 3rd. (1997) Marrow-mesenchyme connections in the fetal and newborn tympanum. A new entity, *Ann Otol Rhinol Laryngol*, 106 (6), 466-470.
- Lo, W. W., Daniels, D. L., Chakeres, D. W., Linthicum, F.H. Jr, Ulmer, J. L., Mark, L. P., Swartz, J. D. (1997) The endolymphatic duct and sac, *Am J Neuroradiol*, 18 (5), 881-887.
- Mansour, S., Nicolas, K., Ahmad, H.H. (2011) Round window otosclerosis: radiologic classification and clinical correlations, *Otol Neurotol*, 32 (3), 384-392.
- Marsot-Dupuch, K., Gayet-Delacroix, M., Elmaleh-Bergès, M., Bonneville, F., Lasjaunias, P. (2001) The petrosquamosal sinus: CT and MR findings of a rare emissary vein, *Am J Neuroradiol*, 22 (6), 1186-1193.
- Mazziotti, S., Racchiusa, S., Settineri, N., Vinci, S., Salamone, I., Pandolfo, I. (2011) Head and neck radiology: role of multidetector computed tomography in the evaluation of the tympanic canaliculus, *Radiol Med*, 116 (4), 657-666.

- Nomiya, S., Kariya, S., Nomiya, R., Morita, N., Nishizaki, K., Paparella, M. M., Cureoglu, S. (2014) Facial nerve canal dehiscence in chronic otitis media without cholesteatoma, *Eur Arch Otorhinolaryngol*, 271 (3), 455-8.
- Ottaviano, G., Calzolari, F., Martini, A. (2007) Goldenhar syndrome in association with agenesis of the internal carotid artery, *Int J Pediatr Otorhinolaryngol*, 71 (3), 509-512.
- Ozaki, A., Haginomori, S. I., Ayani, Y., Ichihara, T., Inui, T., Jin-Nin, T., Inaka, Y., Kawata, R. (2020) Facial nerve course in the temporal bone: anatomical relationship between the tympanic and mastoid portions for safe ear surgery, *Auris Nasus Larynx*, 47 (5), 800-806.
- Palabiyik, F. B., Hacikurt, K., Yazici, Z. (2017) Facial nerve anomalies in paediatric cochlear implant candidates: radiological evaluation, *J Laryngol Otol*, 131 (1), 26-31.
- Priner, R., Freeman, S., Perez, R., Sohmer, H. (2003) The neonate has a temporary conductive hearing loss due to fluid in the middle ear, *Audiol Neurootol*, 8 (2), 100-110.
- Roll, J. D., Urban, M. A., Larson, T. C. 3rd, Gailloud, P., Jacob, P., Harnsberger, H. R. (2003) Bilateral aberrant internal carotid arteries with bilateral persistent stapedia arteries and bilateral duplicated internal carotid arteries, *Am J Neuroradiol*, 24 (4), 762-765.
- Sanghan, N., Chansakul, T., Kozin, E. D., Juliano, A. F., Curtin, H. D., Reinshagen, K. L. (2018) Retrospective review of otic capsule contour and thickness in patients with otosclerosis and individuals with normal hearing on CT, *Am J Neuroradiol*, 39 (12), 2350-2355.
- Sano, M., Kaga, K., Mima, K. (2007) MRI findings of the middle ear in infants. *Acta Otolaryngol*, 127 (8), 821-824.
- Santos, S., Sgambatti, L., Bueno, A., Albi, G., Suárez, A., Domínguez, M. J. (2010) Hipoacusia en niños con acueducto vestibular dilatado. Estudio de 55 casos, *Acta Otorrinolaringol Esp*, 61 (5), 338-344.
- Sarioglu, F. C., Pekcevik, Y., Guleryuz, H., Olgun, Y., Guneri, E. A. (2019) Variations of the vascular canals in the cochlear implant candidates, *Int J Pediatr Otorhinolaryngol*, 123, 123-127.
- Sennaroglu, L., Tahir, E. (2020) A novel classification: anomalous routes of the facial nerve in relation to inner ear malformations, *Laryngoscope*, 130 (11), E696-E703.
- Shim, H. J., Song, S. J., Chung, K. W., Yoon, S. W. (2014) Petrosquamosal sinus discovered during mastoidectomy, and its radiologic appearance on temporal bone CT: case report and brief review, *Ear Nose Throat J*, 93 (7), E29-32.
- Tekdemir, I., Aslan, A., Elhan, A. (1999) The subarcuate canaliculus and its artery - a radioanatomical study, *Ann Anat*, 181 (2), 207-211.
- Terao, K., Cureoglu, S., Schachern, P. A., Paparella, M. M., Morita, N., Sato, T., Mori, K., Murata, K., Doi, K. (2011) Marrow-middle ear connections: a potential cause of otogenic meningitis, *Otol Neurotol*, 32 (1), 77-80.
- Thiers, F. A., Sakai, O., Poe, D. S., Curtin, H.D. (2000) Persistent stapedia artery: CT findings, *Am J Neuroradiol*, 21 (8), 1551-1554.
- Yokoyama, T., Iino, Y., Kakizaki, K., Murakami, Y. (1999) Human temporal bone study on the postnatal ossification process of auditory ossicles, *Laryngoscope*, 109, 927-930.

Appendices

Paper presented at the conference "Neuroradiologia dell' orecchio e delle vie uditive", Italian Society of Medical and interventional Radiology (SIRM), Roma, 18/03/2019.

The images reproduced refer to cases handled by the Author during the period of activity carried out at the University Hospital of Ferrara and at the University Hospital of Udine (Italy), unless otherwise indicated in the individual images.